Aust. J. Phys., 1977, **30**, 509–29

A Radio Study of Abell Clusters

B. Y. Mills and D. G. Hoskins

School of Physics, University of Sydney, N.S.W. 2006.

Abstract

A search for radio sources close to 247 clusters of galaxies in the Abell catalogue has been carried out at the Molonglo Radio Observatory at a frequency of 408 MHz. A list of 116 sources near 89 clusters is given, identifications have been made and criteria for cluster membership have been established. A cluster luminosity function is derived in the range 10^{23}–10^{25} W Hz^{-1} sr^{-1}, and spectra have been obtained for sources in 25 clusters utilizing published surveys made at other frequencies. It is found that there is no correlation between the richness of a cluster and its inclusion of at least one radio source, but those clusters containing multiple sources are significantly richer than average.

1. Introduction

The Abell (1958) catalogue of clusters of galaxies provides a statistically homogeneous collection of 2712 rich clusters at approximately known distances out to a redshift of $z \approx 0 \cdot 2$. It therefore contains a large sample of galaxies which may be examined for radio emission. In general the clusters are too distant for an effective study of weakly emitting 'normal galaxies' and insufficiently numerous to include the rare powerful radio galaxies which comprise the greatest proportion of catalogued radio sources. However, they do include numerous weak radio galaxies which are otherwise difficult to isolate. Additionally, it might be hoped that information about the intergalactic material in clusters may be obtained indirectly.

An investigation of a limited sample of 58 clusters, using the Arecibo reflector supplemented by the Molonglo radiotelescope, has already been described (Mills *et al.* 1968). Here we extend the investigation to a larger group of clusters using the Molonglo radiotelescope alone. In these new observations the sensitivity limit has been extended from about 1 to $0 \cdot 4$ Jy. All clusters south of declination $+18°$ and up to distance class 4 ($z \lesssim 0 \cdot 1$) have been observed, plus a random selection from distance classes 5 and 6 (up to $z \approx 0 \cdot 2$), chosen for observational convenience. Altogether 247 clusters were observed, including 35 of the clusters in the earlier program. The observations were made mainly during the period 1968–70 but final analysis of the results has been unavoidably delayed until recently.

The interpretation of cluster observations is difficult because of the high degree of contamination with distant radio sources of very much greater absolute luminosity than the cluster members. For example, we list 116 sources detected in close proximity to the cluster centres, but statistical considerations imply that nearly half of these may be field sources. In order to confine attention to the cluster members it has been necessary to apply stringent statistical criteria which exclude many of the weaker sources from consideration. Measurement of the redshift of an identified galaxy provides a better criterion of cluster membership but this information is available in very few doubtful cases.

2. Cluster Distances and Intrinsic Source Properties

Since only a small fraction of the clusters in the Abell catalogue contain galaxies with measured redshifts, distances to individual clusters must rely on estimates of apparent magnitude. Rather than assume a particular value for the absolute magnitude of a particular cluster member, Abell's approach will be followed here. This consists of calibrating the estimated apparent magnitude for the tenth brightest cluster members directly in terms of measured redshifts. This method has the advantage that it does not require a specific form of the optical K correction to be assumed, and the results are not affected by any nonlinearity that might exist in the magnitude scale. It does, however, require the clusters for which redshift measurements are available to be a representative sample. In practice there is some bias in favour of 'interesting' clusters, such as those containing strong radio sources, but the available evidence does not suggest there to be any significant effect on the observed $\log z$ versus m_{10} relationship (Rowan-Robinson 1972).

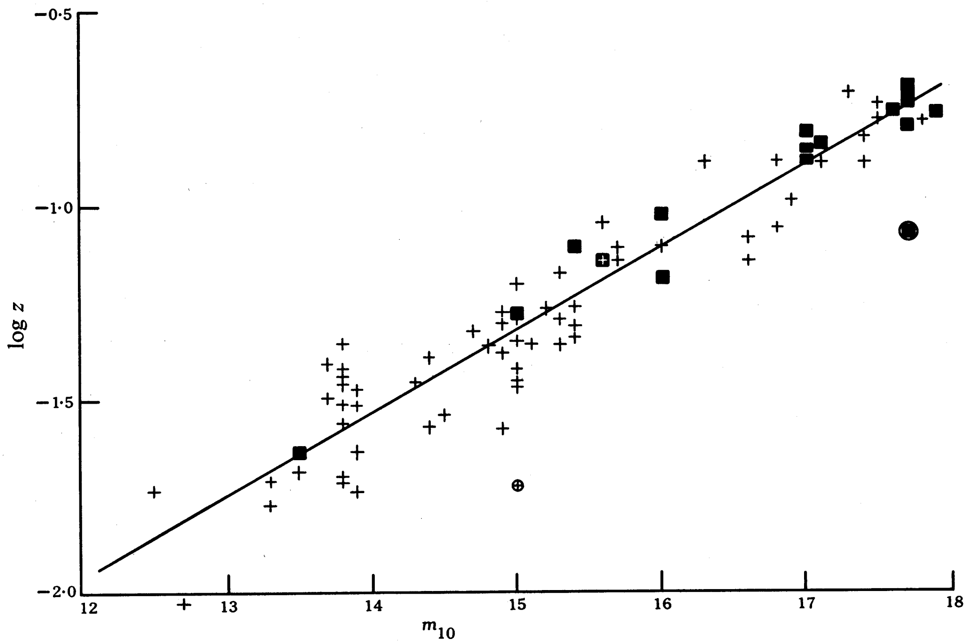

Fig. 1. Least square calibration line for the cluster distance scale using current redshift data. Points available to Abell are shown as squares. The two circled points were excluded from the least square calculation.

Fig. 1 is a redshift–apparent-magnitude scatter diagram for 85 Abell clusters for which redshift measurements are available. The optical magnitudes m_{10} refer to the tenth brightest cluster member and are taken from Abell's catalogue. Most of the redshift data are taken from a list compiled by Noonan (1973) who gave references to the original measurements. Eight of the points correspond to the following clusters not included in Noonan's list:

Abell No.	m_{10}	z	Abell No.	m_{10}	z
98	16·9	0·1028	2029	16·0	0·0777
274	16·3	0·1289	2224	17·4	0·1499
655	17·1	0·1287	2589	15·3	0·0440
665	17·5	0·1832	2670	15·7	0·0774

These data are taken from Sargent (1973), except for A2589, where they are from Sandage (1972).

The straight line shown in Fig. 1 is the result of a least squares fit to the data. Two points (circled in Fig. 1) which lie more than three standard deviations from the line were omitted from the calculation. These correspond to A465 and A1318. Many of the redshift values listed by Noonan (1973) are average values for several cluster members measured by several observers. All points, however, were given equal weight in the least squares calculation, since it is magnitude, rather than the redshift which is responsible for most of the scatter in the diagram.
The equation of the line is

$$\log z = 0{\cdot}2126\, m_{10} - 4{\cdot}513\,. \tag{1}$$

The r.m.s. deviation of the points about the line is 0·09 in $\log z$, corresponding to 23% in z, or 0·4 magnitudes in m_{10}. The inclusion of a term in m_{10}^2 does not significantly improve the fit. This confirms the result of Rowan-Robinson (1972), based on 31 clusters, that a straight line is adequate to represent the $\log z$ versus m_{10} relationship rather than the curve suggested by Abell's original data. Any departure from a straight line or from the 'ideal' slope of 0·2 is not of any significance, since repeatability, rather than absolute accuracy, was the principal aim in setting up the magnitude scale. Although the dispersion is somewhat greater than for the data used by Abell (rejecting one discrepant point) or by Rowan-Robinson (1972), the relationship (1) is considered to be the most reliable available for estimating redshifts from the values of m_{10} in Abell's catalogue.

More recent work by Abell (1972) and Bautz and Abell (1973) suggests that the quantity m^*, the magnitude at which the integrated optical luminosity function changes slope, may be a better distance indicator (in the sense of yielding a smaller dispersion about the $\log z$ versus m_{10} relationship). However, values of m^* are not available for sufficient clusters to take advantage of the smaller dispersion.

One of the three points which Rowan-Robinson (1972) excluded from his calculations corresponds to a redshift of 0·237 for the cluster A1890. This redshift is the value measured for the galaxy IC 5532, which lies approximately 2·5° north of the cluster. The association of the redshift with the Abell cluster probably results from the fact that both IC 5532 and A1890 have previously been suggested as being associated with the radio source 3C 296.

In order to calculate intrinsic properties of cluster sources as a function of the redshift, it is necessary to choose a particular cosmological model. Here, the convenient Einstein–de Sitter model is adopted, which has the following relationships between intrinsic and observed properties:

$$d = \theta(2c/H_0)(1+z)^{-1}\{1-(1+z)^{-\frac{1}{2}}\}\,, \tag{2}$$

$$P_{408} = S_{408}(2c/H_0)^2(1+z)^{\alpha+2}\{1-(1+z)^{-\frac{1}{2}}\}^2\,, \tag{3}$$

where d is the projected separation corresponding to an angular separation θ, and P_{408} ($\mathrm{W\,Hz^{-1}\,sr^{-1}}$) is the luminosity corresponding to a flux density S_{408} at 408 MHz. In our calculations, the mean spectral index α is taken as $-0\cdot 9$ (Murdoch 1976) and the Hubble constant H_0 is taken as $100\,\mathrm{Km\,s^{-1}\,Mpc^{-1}}$ for consistency with previous radio investigations.

3. Observations and Identifications

The 247 clusters selected for observation are listed in Table 1, together with values of the red magnitude m_{10} of the tenth brightest galaxy, the distance class D, and the richness class R. These data have been taken directly from Abell's catalogue.

The selected clusters were observed at a frequency of 408 MHz using the multiple pencil beam system of the Molonglo radio telescope. The eleven pencil beams, whose half-power beamwidths are $2'\cdot 6$ in right ascension and $2'\cdot 86\sec(\delta+35°\cdot 5)$ in declination, lie in the plane of the meridian, spaced at intervals of one half-beamwidth, and thus cover a declination range of $14'\cdot 3\sec(\delta+35°\cdot 5)$ in a single scan. For some of the nearer clusters, several scans at different declination settings were necessary to cover the cluster out to the required angular separation from the cluster centre. Clusters near which a source was detected were reobserved in order to reduce the errors in position and flux density.

The system used for recording and analysing the data was similar to that described earlier. For sources which were unresolved, the positions and flux densities were obtained using the point source fitting program described by Munro (1971). For sources showing slight extension, the degree of extension was measured on analogue records, and a correction was then applied to the fitted flux density. For well-resolved sources, centroid positions and integrated flux densities were determined from a printout of the digital data.

The observations were taken from a number of observing sessions. Since the telescope's sensitivity and the reliability of the position calibration vary from session to session, the positional errors cannot be expressed as a function of flux density. For each source the radio position has been assigned to an error classification denoted by A, B or C. Approximate standard errors corresponding to these classifications are as follows:

	A	B	C		A	B	C
σ_α	3″	5″	10″	σ_δ	5″	8″	12″

All clusters near which a radio source was detected were examined on the Palomar Sky Survey prints and any objects considered to be possible identifications were selected for optical measurements. For these measurements, usually six reference stars were used for each field, and the final accuracy achieved is $\sim 1''$ in each coordinate. (The errors may be slightly larger than this in the case of bright galaxies, due to inaccuracies in setting the cross wires on the overexposed images on the Sky Survey prints.) Optical objects measured in this way were described according to the following scheme: E, elliptical galaxy; Sp, spiral galaxy; DB, double galaxy; CG, compact galaxy; G, galaxy (not classified); QSO, optically confirmed QSO; BSO, blue stellar object; ST, stellar image (other than QSO and BSO).

Stellar objects lying close to a radio position, even though not considered to be possible identifications, were also measured and recorded if sufficiently close. In addition, the position of the brightest or the second brightest cluster member

Table 1. Abell clusters observed

Abell No.	m_{10}	D	R	Abell No.	m_{10}	D	R
2	17·3	6	1	389	15·9	4	2
13	16·6	5	2	397	15·1	3	0
14	15·2	3	0	399	15·6	3	1
18	17·1	5	0	400	13·9	1	1
20	17·1	5	1	401	15·6	3	2
35	17·1	5	1	415	16·3	4	1
43	15·9	4	0	419	15·7	4	0
66	17·8	6	0	428	16·5	5	0
74	15·9	4	0	438	17·2	5	1
76	15·0	3	0	440	17·2	5	1
85	15·7	4	1	458	17·2	5	2
86	15·9	4	0	465	17·7	6	1
88	15·6	3	1	470	16·9	5	0
99	17·1	5	0	471	17·6	6	1
102	15·4	3	0	474	17·1	5	1
114	15·9	4	0	477	17·5	6	1
116	15·7	4	0	487	17·0	5	1
117	16·0	4	0	495	17·0	5	0
119	15·0	3	1	496	15·3	3	1
121	16·0	4	1	500	15·8	4	1
133	15·9	4	0	506	17·5	6	2
134	16·0	4	0	513	17·5	6	0
147	15·0	3	0	514	15·2	3	1
151	15·0	3	1	524	16·7	5	1
154	15·6	3	1	526	16·4	4	1
158	15·9	4	0	533	15·8	4	0
166	16·3	4	1	535	17·4	6	1
168	15·4	3	2	538	17·4	6	1
171	15·9	4	0	539	14·4	2	1
189	15·7	4	1	543	16·9	5	1
193	16·0	4	1	547	17·0	5	2
194	13·9	1	0	548	13·7	1	1
208	16·6	5	0	550	16·7	5	2
224	17·0	5	1	551	17·5	6	1
225	15·9	4	1	592	15·0	3	1
235	17·5	6	1	598	17·4	6	1
240	15·6	3	0	614	17·0	5	0
245	16·4	4	0	619	16·8	5	1
246	16·4	4	1	632	17·2	5	1
274	16·3	4	3	638	17·0	5	0
277	15·6	3	1	644	16·2	4	0
295	16·6	5	1	653	17·0	5	1
316	17·2	5	0	658	17·0	5	1
336	17·2	5	0	673	17·1	5	0
342	17·7	6	1	674	17·7	6	0
357	16·8	5	0	688	17·5	6	1
358	15·6	3	0	689	17·1	5	0
362	17·7	6	1	703	17·8	6	1
365	17·4	6	0	713	16·8	5	0
371	17·0	5	1	744	16·6	5	0

Table 1 (*Continued*)

Abell No.	m_{10}	D	R	Abell No.	m_{10}	D	R
754	15·2	3	2	1644	15·7	4	1
769	16·5	5	1	1648	16·9	5	1
776	17·9	6	1	1651	16·0	4	1
780	16·6	5	0	1663	17·0	5	1
838	15·3	3	0	1684	17·2	5	1
858	16·6	5	0	1692	17·2	5	0
878	16·8	5	1	1709	16·4	4	0
912	15·9	4	0	1729	17·2	5	1
933	15·9	4	0	1736	14·8	2	0
957	15·9	4	1	1750	15·9	4	0
970	16·5	5	1	1768	17·2	5	0
978	15·6	3	1	1772	17·0	5	1
979	15·3	3	0	1773	15·6	3	1
993	14·9	3	0	1780	16·6	5	1
999	15·6	3	0	1796	17·2	5	1
1016	15·4	3	0	1809	15·8	4	1
1020	16·0	4	1	1833	17·0	5	1
1032	15·7	4	0	1836	15·7	4	0
1060	12·7	0	1	1837	15·7	4	1
1069	15·1	3	0	1860	17·2	5	1
1113	17·6	6	1	1866	17·2	5	1
1126	16·0	4	1	1881	17·0	5	1
1139	15·0	3	0	1890	15·5	3	0
1142	15·4	3	0	1897	17·0	5	0
1145	15·7	4	0	1899	16·0	4	0
1149	16·0	4	0	1913	16·0	4	1
1171	16·2	4	0	1924	17·0	5	2
1183	17·2	5	1	1970	17·2	5	1
1205	16·9	5	1	1983	15·4	3	1
1216	16·0	4	1	1991	15·4	3	1
1238	16·0	4	1	2020	16·0	4	0
1308	15·7	4	0	2028	15·7	4	1
1332	16·0	4	0	2029	16·0	4	2
1334	15·7	4	0	2033	15·7	4	0
1362	16·0	4	0	2036	16·0	4	0
1364	16·0	4	1	2040	15·7	4	1
1390	16·0	4	0	2048	16·0	4	1
1399	16·0	4	2	2052	15·0	3	0
1469	17·2	5	2	2055	16·0	4	0
1474	16·0	4	1	2063	15·1	3	1
1516	16·6	5	1	2066	17·2	5	2
1524	17·2	5	2	2072	17·0	5	0
1541	16·0	4	1	2082	17·0	5	0
1564	16·6	5	0	2094	16·7	5	1
1581	17·2	5	1	2108	15·7	4	0
1604	17·6	6	1	2113	17·1	5	0
1612	17·6	6	0	2147	13·8	1	1
1620	17·2	5	0	2151	13·8	1	2
1625	17·0	5	0	2152	13·8	1	1
1631	15·4	3	0	2159	15·9	4	0

Table 1 (*Continued*)

Abell No.	m_{10}	D	R	Abell No.	m_{10}	D	R
2163	17·5	6	2	2480	16·9	5	1
2173	17·1	5	1	2504	17·2	5	0
2182	17·4	6	0	2511	16·0	4	0
2204	17·1	5	3	2525	16·0	4	0
2324	16·8	5	1	2549	17·0	5	1
2328	16·4	4	2	2571	17·6	6	1
2331	16·3	4	0	2572	15·3	3	0
2338	17·0	5	1	2589	15·3	3	0
2347	16·4	4	1	2593	15·1	3	0
2350	17·1	5	0	2612	17·7	6	2
2353	16·8	5	1	2623	17·2	5	3
2361	16·7	5	1	2630	15·2	3	0
2362	16·9	5	1	2644	16·6	5	1
2366	15·9	4	0	2656	16·2	4	0
2382	16·0	4	1	2657	14·9	3	1
2384	15·9	4	1	2660	16·4	4	0
2398	17·1	5	0	2665	15·8	4	0
2399	15·6	3	1	2670	15·7	4	3
2410	16·0	4	1	2675	16·4	4	1
2412	15·9	4	0	2676	16·8	5	0
2415	15·9	4	0	2700	16·0	4	1
2448	16·0	4	0	2709	17·2	5	1
2457	16·0	4	1				
2459	16·0	4	0				
2462	16·2	4	0				

(whichever was the nearer to the radio position) was also recorded if it had not already been measured. As a rough indication of brightness, the red magnitudes of galaxies and the photographic magnitudes of stellar objects were estimated to the nearest magnitude.

Assigning an identification to a radio source in a relatively close cluster, such as an Abell cluster, presents some problems because it is usually not known whether possibly associated galaxies are actually cluster members. If it is physically located in the cluster, angular displacements between the parent galaxy and the radio source due to separation of the centroids may be quite large, substantially exceeding the positional uncertainties (see e.g. Mills *et al.* 1968). If it is a field source it is likely to be considerably more distant than the Abell cluster, so that angular displacements are more likely to be dominated by measurement errors. To overcome this problem and for some other purposes described later, the radio sources have been divided into three statistical categories which are related to their probable association with a cluster. A Category I source is situated within a critical angle θ_c, corresponding to a projected linear distance of 400 kpc from the cluster centre, and has a flux density greater than a critical value S_c corresponding to the flux density above which the probability of a chance association within θ_c is 0·02. A Category II source is situated within a projected distance of 700 kpc, but not included in Category I, while the remainder of the sources are assigned to Category III. Some illustrative examples of the magnitude of θ_c and S_c are tabulated below; the general relations being given in the Appendix:

z	0·05	0·10	0·15
θ_c	10′·0	5′·4	3′·9
S_c	1·12	0·49	0·32 Jy

In searching for identifications with galaxies, the Category I sources were provisionally assumed to be associated with the clusters, and galaxy identifications were sought to an angular separation corresponding to a projected distance of 50 kpc at the cluster redshift. Association of the clusters with Category II sources is uncertain, while association with Category III sources is unlikely, as is discussed below. Identifications with Category II and III sources have been sought on the assumption that they are field sources, and the angular displacement criteria of Schilizzi (1975) have been employed. These criteria are based on combining a physical displacement, which is a function of galaxy magnitude, with the measurement errors; they are more stringent than the criterion used for the Category I identifications.

Some possible and known associations with QSOs, BSOs and neutral stellar objects have also been noted; these are based on angular displacements less than twice the standard erorrs in position.

4. Table of Results

Details of the radio sources observed near 89 clusters are given in Table 2. For each source the following information is given:

Column 1, Abell catalogue number of cluster.

Column 2, redshift z, calculated according to equation (1).

Column 3, source reference number in the Parkes and Molonglo systems.

Column 4, right ascension α of the radio source (epoch 1950·0).

Column 5, declination δ of the radio source (epoch 1950·0).

Column 6, error class Δ as described in Section 3. Where no error class is given, the listed position is the approximate centroid of an extended or double source.

Column 7, 408 MHz flux density S_{408} on the Wyllie (1969) scale.

Column 8, source structure Σ. No entry indicates that the source is unresolved. 'X' indicates that the source noticeably broadens the response pattern of the radiotelescope. 'D' indicates that the source contains two components and, when no reference number is quoted in column 3, two of the separately listed sources in the cluster have been regarded as components of a double source with the centroid given. 'XD' indicates that the source is clearly extended and appears to contain two components which may be only partially resolved. In one instance 'T' is used to designate the centroid of three close separately listed sources regarded as a triple. The separate sources included in the double or triple sources may be determined from inspection of column 7, where the flux densities have been added together.

Column 9, angular separation θ of the source position from the nominal cluster centre.

Column 10, statistical category as described in Section 3.

Table 2. Properties of radio sources detected near Abell clusters

(1) Abell No.	(2) z	(3) Source No.	(4) α (1950) h m s	(5) δ (1950) ° ′ ″	(6) Δ	(7) S_{408} (Jy)	(8) Σ	(9) θ ′	(10) Category	(11) L	(12) Optical Ident.	(13) Optical Posn	(14) Notes
2	0·146	0005−199	00 05 43	−19 56 40		1·80	X	3·1	I	1·54	**16*E**	1P 14N	B
13	0·104	0010−197	00 10 55·2	−19 46 26	C	0·50		2·6	I	0·68	**17 G**	25P 20S	2B is 1′·6NF
66	0·187	0034−054	00 34 09·0	−05 29 36	B	0·54		1·8	I	1·23	**17 G**	0 17S	B
85	0·067	0038−096	00 38 58·5	−09 39 00	A	1·47		2·1	I		**19 G?**	7F 2N	
		0039−095	00 39 17·6	−09 34 02	C	0·30		4·9	II		**18 E**	2F 9S	
											14 E	13F 36S	B
86	0·074	0039−222	00 39 42·0	−22 13 27	C	0·51		9·4	II				2B is 11′NF
117	0·077	0052−101	00 52 16·7	−10 09 10	B	0·57		20·1	III		**20 BSO**	1F 1S	
		0053−101	00 53 05·6	−10 08 30	A	1·00		11·2	II		20 G?	7F 1S	B is 7′·7SF
											18 G	54P 2S	
119	0·047		00 53 25	−01 37 55		3·5	X	8·2			**14*E**	65F 96N	See map SM
			00 53 51	−01 33 20		4·5	X	1·5			**14*E**	7F 71N	B is 2′·8NP
		0053−015	00 53 40	−01 35 20		8·0	D	3·9	I	1·19	**17*G**	39P 50S	Alternative identifications appear equally permissible
133	0·074	0100−221	01 00 14·7	−22 08 42	A	2·71		4·7	I	1·11	**15 E**	5F 20S	B
158	0·074	0108+165	01 08 00·0	16 34 00	C	0·77		16·1	III		**15 E**	17P 21S	Not cluster member; B is 16′F
194	0·028	0123−016	01 23 30	−01 37 30		13·6	XD	11·3	I	0·96	**13*DB**	54P 95N	B; see map SM
208	0·104	0128+002	01 28 59·7	00 17 59	A	1·49		0·1	I	1·15	**16 E**	12P 3S	B
224	0·126	0134−071	01 34 29·5	−07 11 35	B	0·54		19·5	III				
		0135−071	01 35 48·0	−07 10 30	B	0·59		2·5	I	0·92	**17 G**	6F 5S	B
235	0·161	0137−177	01 37 59·0	−17 44 34	A	1·72		4·4	II	1·60	**17*E**	14P 5N	B
240	0·064	0138+073	01 38 00·3	07 22 01	B	0·95	X	19·3	III				B is 18′F
		0138+074	01 38 18·0	07 28 19	C	0·50		15·8	III		19 BSO	15P 6N	Extended 1′EW
357	0·114	0226+129	02 26 11·4	12 57 06	B	1·16		8·9	III				B is 10′·6NF
362	0·178	0229−051	02 29 09·9	−05 06 11	B	0·68		1·0	I	1·29	**17 G**	16F 0	B
400	0·028	0255+058	02 55 05	05 50 45		16·3	X	1·5	I	1·04	**13*DB**	[28P 85S	B
												30P 69S]	18^m E galaxy (105F, 24N) may also radiate
401	0·064	0255+133	02 55 45·8	13 21 40	B	1·05		6·5	I	0·57	**20*G**	13P 95S	
											17*G	19F 42N	B is 6′·7NF

Table 2 (*Continued*)

(1) Abell No.	(2) z	(3) Source No.	(4) α (1950) h m s	(5) δ (1950) ° ′ ″	(6) Δ	(7) S_{408} (Jy)	(8) Σ	(9) θ ′	(10) Cate-gory	(11) L	(12) Optical Ident.	(13) Optical Posn	(14) Notes
415	0·090	0304−122	03 04 35	−12 17 30		3·80	X	3·7	I	1·43	16*E	82P 24S	2B; B is 10′·9N
											17*E	8F 46N	Perhaps both galaxies radiating
474	0·133	0405−167	04 05 30·9	−16 46 26	B	0·64	X	3·8	I	1·00	17 G	18F 1S	2B; may be extended EW; B is 15′P
		0406−167	04 06 38·7	−16 47 37	A	1·44		15·2	III				
496	0·055	0431−133	04 31 17	−13 21 45		0·89	X	0·3	II	0·27	13 E	25F 11S	B
		0431−134	04 31 52	−13 28 50		2·40	D	10·7	II		16 CG	7P 27N	
		0431−132	04 31 57	−13 16 33		5·50	X	11·0	II		17 G	44P 22N	
506	0·161	0440−096	04 40 31·6	−09 41 01	C	0·43		9·7	III		17 G	1P 4N	B? is 7′·9S
514	0·052	0445−206	04 45 23	−20 38 20		0·40	X	6·5	II		15*E	44F 101S	2B; possible 'head–tail' source; see Map SM
		0445−205	04 45 53	−20 32 30		0·95	XD?	5·4	II		18*G	13F 6S	
		0446−206	04 46 20	−20 37 40		2·70	X	13·0	II		17*E	10P 15N	
526	0·094	0457+052	04 57 04·0	05 15 32	C	0·65	X	7·7	II		18 G	5F 15S	~2′EW; galaxy is almost obscured by a star; may be 2B; a 20^m G is closer to radio position
		0457+054	04 57 22·1	05 24 55	C	0·40		3·2	II		17 G	19F 20S	B is 3′·2S
551	0·161	0552−176	05 52 55·2	−17 39 17	B	0·45	X	7·4	III		18 BSO	5P 16N	Slightly extended EW; B is 9′·2SP
614	0·126	0758+181	07 58 14·3	18 07 01	B	1·34	X	0·5	I	1·28	17 E	0 3N	B; extended ~1′EW
619	0·114	0759−020	07 59 05·6	−02 00 54	C	0·54	X	15·6	III		19 G	5F 15S	Slightly extended EW; B is 15′F
											20 BSO	14F 18S	
658	0·126	0821+157	08 21 12·4	15 44 37	B	0·79		7·0	II	1·05	16 DB	18P 8S	B
688	0·161	0834+159	08 34 03·4	15 56 35	C	0·42		10·7	III		18 BSO	25F 8S	
744	0·104	0903+169	09 03 44·0	16 58 17	A	6·21		12·7	III		18·3*QSO	1F 1S	Data from Hunstead (1971, 1972)
754	0·052		09 05 59·1	−09 21 34	B	0·60		8·2			18 G	14P 5S	
											17 G	1F 11N	
			09 06 22·8	−09 28 40	C	0·50		1·7			18 CG	49P 6N	
		0906−094	09 06 10	−09 24 50		1·10	D	4·1	I	0·43	13 E	53P 46S	B; galaxy lies close to line joining the two components
		0907−093	09 07 53·3	−09 23 00	A	0·80		22·4	III				
780	0·104	0915−118	09 15 41·2	−11 53 07	A	138	X	12·5	III		15*D	0 3N	Hydra A is not associated with A780
838	0·055	0933−047	09 33 45·7	−04 42 04	C	0·42		13·5	II	0·04	15 DB	16F 39S	B
878	0·114	0947+060	09 47 48·8	06 05 49	C	0·38		11·7	III		18 ST	0 12N	Bis 5′·0SP
		0948+060	09 48 26·7	06 04 52	C	0·55		20·4	III		17 CG	6F 10N	

(1) Abell No.	(2) z	(3) Source No.	(4) α (1950) h m s	(5) δ (1950) ° ′ ″	(6) Δ	(7) S_{408} (Jy)	(8) Σ	(9) θ ′	(10) Category	(11) L	(12) Optical Ident.	(13) Optical Posn	(14) Notes
912	0·074	0957+003	09 57 43·7	00 19 49	A	2·88		16·8	III		**17·6*QSO**	0 0	Data from Hunstead (1971, 1972)
933	0·074	1005+007	10 05 37·4	00 44 37	A	0·99		8·0	II		**16 E**	21F 11N	2B is 3′·4NF
1069	0·050	1036−082	10 36 15·6	−08 15 56	C	0·44		17·7	III		18 CG	17P 24S	B is 17′SF
1139	0·047	1055+018	10 55 55·4	01 50 03	A	4·3		6·9	I		**18*QSO**	1P 1N	Data from Hunstead (1971, 1972)
1142	0·058	1058+110	10 58 10·6	11 02 17	B	1·71		13·4	II		**18*QSO**	2F 4N	Nearest galaxy is spiral 2·4′S; B is 13′S
		1059+107	10 59 40·7	10 45 17	A	3·50		20·6	III		18 ST	2F 5N	
1145	0·067	1059+169	10 59 12·6	16 56 38	B	0·89		5·6	I	0·54	**16 E**	5F 8N	Brightest spiral is 4′S; brightest elilptical is 8′·8SF
1149	0·077	1059+078	10 59 26·1	07 52 32	B	0·71		14·4	III		19 G	7P 26S	2B is 12′·6F
1171	0·085	1104+030	11 04 31·9	03 03 36	C	0·52		10·9	III				
1238	0·077	1120+013	11 20 19·6	01 23 14	B	0·58		1·1	II	0·48	**15 E**	10F 6N	B
											15 E	25F 6N	2B
1308	0·067	1130−037	11 30 30·7	−03 44 41	B	2·30	X	4·2	I	0·95	**15 E**	17F 26N	B; extended ~2′·5NS
1469	0·139	1202−069	12 02 45·7	−06 59 16	C	0·48		10·5	III				B is 10′·9NF
		1203−069	12 03 58·3	−06 58 05	A	1·88		13·5	III				B is 14′·2NP
1485	0·169	1208−035	12 08 37·2	−03 33 35	C	0·39		5·4	II		20 G?	13P 12S	B is 1′·9F
1516	0·104	1216+055	12 16 18·5	05 31 21	A	1·36		1·4	I	1·11	**17 E**	9F 3N	B
1604	0·169	1242−227	12 42 08·6	−22 47 26	C	0·29		11·9	III				
1620	0·139	1247−012	12 47 28·9	−01 16 12	B	0·84		5·1	II	1·16	**16 E**	13F 6N	B
1631	0·058	1250−150	12 50 16·2	−15 03 47	B	0·75		6·3	II		**16 E**	29F 29S	B is 4′·7S
1644	0·067	1253−171	12 53 58·7	−17 06 50	C	0·47		9·0	II		**18 G**	12P 14N	2B is 6′·7NF
1684	0·139	1306+107	13 06 35·4	10 45 27	A	1·63		3·8	I	1·45	**16*E**	15P 7N	B
1736	0·043	1323−268	13 23 59·1	−26 51 51	B	0·72		1·5	II		**16 E**	17F 16N	B is 16′·2SF
1772	0·126	1339−108	13 39 26·4	−10 51 32	B	0·72		0·8	I	1·01	**16 E**	1P 10S	B
		1340−107	13 40 14·9	−10 45 54	C	0·39		13·5	III		**16 E**	7P 4N	
1833	0·126	1356+048	13 56 56·3	04 48 53	C	0·44		11·8	III				B is 12′·7F
1836	0·067	1358−113	13 58 59	−11 21 50		4·40	D	1·2	I	1·23	**13*E**	35F 8S	B; see map SM

Table 2 (*Continued*)

(1) Abell No.	(2) z	(3) Source No.	(4) α (1950) h m s	(5) δ (1950) ° ′ ″	(6) Δ	(7) S_{408} (Jy)	(8) Σ	(9) θ ′	(10) Category	(11) L	(12) Optical Ident.	(13) Optical Posn	(14) Notes
1890	0·061	1415+084	14 15 03·5	08 26 38	B	0·87		1·7	I	0·44	18 GG	0 8S	B is 2′·5SF
1899	0·077	1419+180	14 19 31·2	18 02 34	B	1·51		9·9	II		18 DB	34F 14S	B is 4′·5SP
1913	0·077	1424+169	14 24 40·6	16 56 41	C	0·49		3·8	II		18*BSO	5F 2S	B is 10′·1P; nearest galaxy is 0′·8SP
2029	0·077	1508+059	15 08 27·3	05 55 55	A	2·66		1·3	I	1·14	13 D	0 6N	B
2033	0·067	1508+065	15 08 59·3	06 32 05	A	1·67		0·9	I	0·81	15 E	15P 8N	B is 0′·8P; either identification is possible
2036	0·077	1508+182	15 08 50	18 15 00		2·30	X	5·2	I	1·08	16 E	16F 110S	Possible 'head–tail' source; B is 8′·4SF
2048	0·077	1511+045	15 11 26·1	04 32 14	B	1·15		20·6	III		19 BSO	3F 10S	
		1512+046	15 12 04·4	04 36 18	C	0·70	X	10·9	II		17 E	41P 17N	Ext ~ 1′EW
											20 G	3P 2N	
		1512+045	15 12 40·8	04 35 11	C	0·47		1·8	II		15 E	63F 3N	B
2052	0·047	1514+072	15 14 16·9	07 12 13	A	28·0		0·3	I	1·74	16*E	2F 3N	B; optical data from Hunstead (1971)
2055	0·077	1516+064	15 16 19·0	06 24 57	A	1·23		1·0	I	0·81	17 CG	21P 8S	2B is 8′·8SF
2072	0·126	1523+184	15 23 10·2	18 24 11	C	0·41		6·1	II				B is 4′·6F
2082	0·126	1528+036	15 28 42·1	03 41 20	C	0·28		8·7	III				B is 8′·4P
		1529+036	15 29 04·6	03 36 11	C	0·38		13·1	III				B is 14′·7P
2094	0·109	1533−017	15 33 11	−01 44 00		0·71	X	14·9	III		18 CG	1P 21N	
		1533−018	15 33 40	−01 50 40		0·37	X	5·2	II				
		1533−019	15 33 53	−01 55 00		0·42	X	3·5	II		17 E	38F 15S	2B
		1534−018	15 34 08	−01 51 30		0·61	X	2·1	I	0·80	17 G	36P 5S	
			15 33 56	−01 52 20		1·40	T	1·1					Centroid of the three close sources above; B is 4′·3N
2108	0·067	1538+182	15 38 48·9	18 15 46	C	0·73		19·3	III				B is 18′SP
2147	0·026		15 59 07·2	15 45 20	A	2·26		21·7			15*E	88P 87S	
			16 00 20·1	15 52 24	A	2·40	X	11·6			15 E	42F 73N	Extended ~ 1′·5EW
		1559+158	15 59 45	15 49 00		4·66	D	14·5	I	0·45	13*DB	85F 61N	B is 17′N
2151	0·026	1602+178	16 02 53·9	17 52 07	A	2·11		1·7	II		14*E	1F 15S	B is 7′·9P
		1603+179	16 03 46·6	17 55 58	C	0·47		11·5	II		19 BSO	2P 15S	
2152	0·026	1603+165	16 03 17·8	16 34 25	C	0·41		2·9	II	−0·61	17 G	15F 1N	B is 1′·2P; either identification is possible
2182	0·154	1620+143	16 20 14·9	14 23 41	B	1·14		11·5	III		18 CG	11P 12S	B is 6′·7SP
2204	0·133	1630+056	16 30 19·8	05 40 35	C	0·37		1·5	I	0·75	14 E	10P 14N	B

(1) Abell No.	(2) z	(3) Source No.	(4) α (1950) h m s	(5) δ (1950) ° ′ ″	(6) Δ	(7) S_{408} (Jy)	(8) Σ	(9) θ ′	(10) Cate- gory	(11) L	(12) Optical Ident.	(13) Optical Posn	(14) Notes
2366	0·074	2139−069	21 39 43·3	−06 57 35	B	1·14		11·0	II		**17 G**	1P 1S	2B is 9′·2SP
2382	0·077	2149−158	21 49 12	−15 51 35		1·40	X	1·9	I	0·86	**16 DB**	[24P 1N	B is 4′·6S
												13P 6S	
2399	0·064	2154−080A	21 54 23·8	−08 04 53	A	0·90		8·0	I	0·50	**15 E**	9P 9N	B
		2154−080B	21 54 56·5	−08 02 05	A	0·89		0·6	I	0·50	**15 E**	22P 7N	
2412	0·074	2201−216	22 01 16·9	−21 41 31	B	0·65		1·7	I	0·49	**17 E**	21F 7N	B
											16 E	16P 4N	
2415	0·074	2203−058	22 03 00·2	−05 50 21	B	0·85		3·1	I	0·60	**16 E**	21F 11N	2B is 3′·4N
2448	0·077	2229−086	22 29 05	−08 40 00		1·90	XD	3·0	I	1·00	**14*E**	9F 1N	B
2457	0·077	2233+010	22 33 41·4	01 04 13	C	0·53		10·6	II		**17 G**	15F 2S	B is 10′NP
2462	0·085	2235−177	22 35 49·8	−17 47 05	A	1·00		13·0	III		**19 G?**	5F 12N	G? is blue
		2236−176	22 36 29·9	−17 36 34	A	4·20		1·5	I	1·43	**15*E**	4F 28N	
2480	0·120	2242−180	22 42 21·3	−18 01 17	C	0·38		15·5	III		**17 CG**	2F 5N	
		2243−178	22 43 17·9	−17 53 22	B	0·84		3·9	I	1·03	**16 E**	6F 2N	B
2525	0·077	2302−110	23 02 06·1	−11 00 38	C	0·49		18·9	III				B? is 12′·8P
2571	0·169	2315−025	23 15 14·0	−02 32 45	C	0·29		11·5	III		20 G?	6F 4S	B is 10′·6NF
		2315−024	23 15 50·9	−02 25 02	C	0·79		8·3	III				
2572	0·055	2316+184	23 16 11·5	18 24 46	C	0·92		5·3	I	0·38	16 E	27P 11N	
											14 E	34F 43N	2B
2593	0·050	2322+143	23 22 02	14 22 30		1·40	XD	0·7	I	0·48	**16 E**	13P 37S	B is 3′·1P
2612	0·178	2328−189	23 28 41·6	−18 57 16	A	1·50	X	5·7	II				Extended ~1′·5EW
2644	0·104	2338−001	23 38 25·9	−00 11 43	A	1·62		2·6	I	1·19	**17*DB**	1F 3S	B is 2′·0NF
		2338−002	23 38 38·3	−00 17 45	C	0·28		6·8	II				B is 7′·9N

Column 11, radio luminosity L, expressed as $L = \log P - 23$. This quantity is only entered when an association with the cluster is probable, i.e. a Category I source identified with a likely cluster galaxy or a Category II source identified with the brightest member of the cluster or another known cluster member. P is calculated from equation (3).

Column 12, optical objects according to the classification scheme described in Section 3. The object listed in boldface type is considered to be the most probable identification; if none is given in boldface, the listed identification is considered to be possible but not probable. Identifications of many of the sources have been suggested previously, sometimes incorrectly, but the poor cross-referencing of southern identifications and the frequent lack of published optical positions leads to a confusing situation which is impractical to resolve here. However, an asterisk is included in the column if we are aware of a previous identification of the source with *any* optical object, not necessarily the identification we have made.

Column 13, optical position with respect to the radio position given in seconds of arc. Abbreviations used are: P, preceding; F, following; N, North; S, South.

Column 14, Notes. Abbreviations used are: B, brightest cluster member; 2B, second brightest member. Positions are given with respect to the radio source. SM refers to Schilizzi and McAdam (1975).

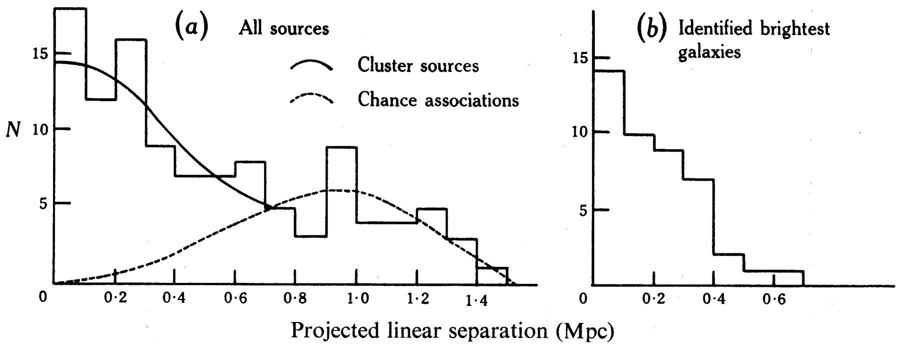

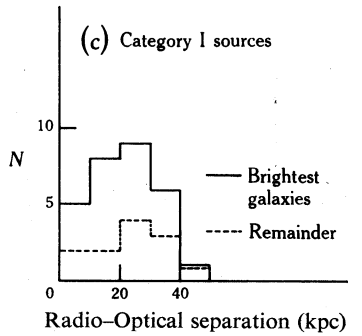

Fig. 2. Distributions for the indicated sources as functions of (*a*) and (*b*) projected linear separation from the nominal cluster centre, and (*c*) radio–optical separation.

5. Statistical Properties

Fig. 2*a* shows the distribution of the projected linear separations between the nominal cluster centres and the tabulated radio source positions. A similar distribution for the sources which have been identified with the brightest cluster galaxy is shown in Fig. 2*b*. The curves in Fig. 2*a* indicate our estimates of the distribution of real cluster sources and chance associations; this division is necessarily subjective, but it is consistent with the distribution in Fig. 2*b* and the expected form of the distribution of chance associations. Few Category I sources represent chance associations (the expectation value is 5) but it seems likely that about half the Category II sources are the result of chance.

As a further check on the Category I sources, similar distributions of the radio-source–galaxy separations are shown in Fig. 2*c* for those sources for which galaxy identifications have been made. Both the brightest and nonbrightest galaxy identifications have distributions of a similar shape, with no evidence for a population proportional to d^2, which would indicate significant numbers of chance associations. In each case the median separation is close to 25 kpc. As this figure also includes the effects of measurement errors, the true median separation will be somewhat less, but probably substantially higher than the equivalent separation in field sources (see e.g. Schilizzi 1975).

Correlation with Cluster Properties

Many clusters have been classified according to their different morphological characteristics but, for the sample observed, only the Abell richness class R (listed in Table 1 for all clusters observed) is available for sufficient clusters to allow meaningful analysis.

The basic dependence of the radio properties of a cluster on the richness class, i.e. the number of galaxies in the cluster, is tabulated below. In this tabulation, the mean richness class is given for clusters containing radio sources in each of the three statistical categories, for clusters containing more than one source in Categories I or II, and for clusters in which no sources were detected.

	I	II	III	Multiple sources	No sources
$\langle R \rangle$	$0{\cdot}67 \pm 0{\cdot}11$	$0{\cdot}65 \pm 0{\cdot}13$	$0{\cdot}52 \pm 0{\cdot}15$	$1{\cdot}18 \pm 0{\cdot}12$	$0{\cdot}67 \pm 0{\cdot}05$

It appears that there is no significant correlation between the richness of a cluster and the probability of occurrence of a radio source, a result which has also been found with varying degrees of significance in previous investigations. However, a new result is that the probability of multiple sources is significantly greater among the rich clusters. A hypothesis consistent with these results is that the potentiality of a galaxy to become a radio galaxy is determined by a property of the primordial gas cloud from which the whole cluster condensed. This 'property' is not related to the mass of the cloud which, however, determines the *number* of potential radio galaxies in a 'radio' cluster.

An obvious 'property' to investigate is the time at which condensation from the primordial cloud occurred. All well-studied radio galaxies are old evolved systems; if radio emission resulted from their own evolution, it would be expected that rich clusters would have a greater probability of containing a radio galaxy because of the natural dispersion in evolutionalry rates. It therefore appears more probable that the determining factor is an actual physical property of the cloud itself at condensation. This may, of course, be dependent on the cosmic time at which the condensation occurred. Some factors which may prove crucial are magnetic fields, turbulent energy or chemical composition. There is obviously scope for an extensive investigation of the overall properties of 'radio' and 'nonradio' clusters to attempt to determine correlations.

6. Cluster Luminosity Function

The term 'cluster luminosity function' is used here to refer to the average number of sources per Abell cluster per unit range of $\log P_{480}$. This function is written ρ_c. Since ρ_c is defined in terms of sources per cluster it cannot be compared directly with the galaxy radio luminosity function, which is defined in terms of sources per unit volume.

Table 3. Data for cluster luminosity function

(1) $\log P-23$	(2) m_{10}	(3) Cluster numbers	(4) Source numbers	(5) ρ_c
0–0·2	13·5	1	0	0
0·2–0·4	14·8	8	1	0·125
0·4–0·6	16·0	88	9	0·102
0·6–0·8	16·8	152	2	0·013
0·8–1·0	17·4	221	7	0·032
1·0–1·2	18·0	247	11	0·045
1·2–1·4	18·0	247	4	0·016
1·4–1·6	18·0	247	4	0·016
1·6–1·8	18·0	247	1	0·004
1·8–2·0	18·0	247	0	0

We consider first all the Category I radio sources which may be reasonably identified with cluster galaxies. For these the luminosity has been calculated and is given in Column 11 of Table 2. To obtain ρ_c it is necessary to determine the number of clusters which would be represented in the table if they did contain sources of given luminosity. For sources in a cluster with redshift z it is shown in the Appendix that the minimum luminosity for inclusion as a Category I source is given by

$$P_{\min} = 2\cdot5\times10^{24}(1+z)^{10/3+\alpha}\{1-(1+z)^{-1/2}\}^{2/3}. \tag{4}$$

This holds out to a distance at which the flux density of a source of luminosity $P_{\min}$ falls below the detection limit. Setting the limit at $S_{408} = 0\cdot4$ Jy (where all detections should be complete), we find the corresponding redshift is $z = 0\cdot12$ ($m_{10} = 17\cdot0$). For greater redshifts we apply equation (3) to determine $P_{\min}$, taking S_{408} as $0\cdot4$ Jy.

The numbers from which the luminosity function is derived are listed in Table 3. Column 1 identifies the luminosity range in intervals of $0\cdot2$ in $\log P$. Column 2 gives the value of m_{10} corresponding to the maximum z for which sources having $\log P$ equal to the mid-point of the luminosity range would be included as a Category I source. Column 3 tabulates the number of clusters in the sample for which m_{10} is equal to or less than the value in Column 2. Column 4 gives the number of Category I radio sources with luminosities in the range defined by Column 1. Finally, in Column 5, ρ_c is tabulated (obtained by dividing the entry in Column 4 by that in Column 3). Because not all the cluster sources are included amongst Category I sources, the true values of ρ_c are some 30%–50% higher.

A similar calculation to the above has been carried out for the identified brightest galaxies labelled B in column 14 of Table 2. In this case P_{min} is determined by equation (3) alone, as no statistical selection has been made. As before, the flux density limit has been taken as 0·4 Jy.

The two sets of results for ρ_c from the Category I sources and the brightest galaxy identifications are:

$\log P - 23$	0–0·4	0·4–0·8	0·8–1·2	1·2–1·6	1·6–2·0
ρ_c for Category I sources	0·125	0·115	0·077	0·032	0·004
ρ_c for brightest galaxies	0·045	0·037	0·060	0·024	0·008

To reduce the scatter, the range of $\log P$ has been increased to 0·4 (one magnitude). It is evident that the cluster luminosity function of the brightest cluster galaxies contains more radio sources of high luminosity and less of low luminosity.

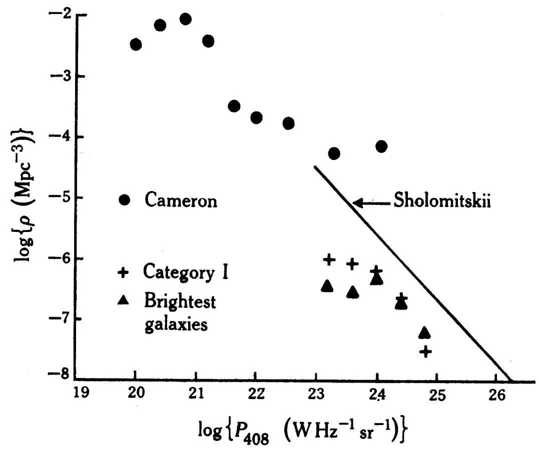

Fig. 3. Radio luminosity functions for identified galaxies in Abell clusters compared with the general radio luminosity functions for galaxies obtained by Cameron (1971) and Sholomitskii (1968*a*, 1968*b*).

In order to compare the present results with the general galactic radio luminosity function, the spatial density of Abell clusters must be estimated. Within a redshift of 0·2 and a solid angle of approximately 6 sr the number of listed clusters is 2172. In an Einstein–de Sitter cosmological model the corresponding space density is approximately 8×10^{-6} Mpc^{-3}. In Fig. 3 the absolute radio luminosity function, obtained by multiplying ρ_c by the cluster space density, is compared with the luminosity function of nearby galaxies obtained by Cameron (1971) and his extrapolation of the luminosity function of radio galaxies obtained by Sholomitskii (1968*a*, 1968*b*). Although statistical uncertainties are large it appears that only a small proportion of the radio sources out to $z \approx 0 \cdot 2$ are to be found in Abell clusters, even after allowing for the underestimation of ρ_c.

7. Radio Spectra

About half of the radio sources which have been associated with a cluster and used to construct the luminosity function have also been catalogued in surveys at other frequencies. Although there is a diversity of absolute flux density scales at low frequencies, reasonably accurate spectral indices may be obtained by making systematic flux density adjustments. The data used are: 80 MHz, Slee and Higgins (1973, 1975); 85 MHz, Mills *et al.* (1958); 178 MHz, Gower *et al.* (1967); 1420 MHz, Ekers (1969), Murdoch (1976); 2700 MHz, Ekers (1969), Bolton *et al.* (1975), Murdoch (1976), Wall *et al.* (1971); 5000 MHz, Bolton *et al.* (1975), Wall *et al.* (1976). Flux density adjustment factors of 1·2 and 1·15 were applied to the 80 and 178 MHz data respectively. The remaining data were used unscaled.

Table 4. Spectral data

Abell number	Source number	S_{80} (Jy)	S_{85} (Jy)	S_{178} (Jy)	S_{408} (Jy)	S_{1415} (Jy)	S_{2700} (Jy)	S_{5000} (Jy)	Indices $-\alpha_-$	$-\alpha_+$
2	0005−199		17		1·80		0·45	0·25	1·43	0·78
85	0038−096	42	56		1·47				2·18	
119	0053−015		70:		8·0D		1·45		1·38:	0·90
133	0100−221	37	35		2·71				1·62	
194	0123−016	32	88		13·6XD	4·4	2·67		0·82	0·87
208	0128+002			2·4	1·49		0·33		0·57	0·80
235	0137−177		10		1·72		0·42	0·30	1·12	0·75
362	0229−051		12:		0·68				1·83	
400	0255+058	51	51		16·3	5·5	3·5		0·71	0·82
401	0255+133				1·05	0·5	0·3			0·65
415	0304−122	10	18:		3·80	1·5	0·82	0·38	0·78:	0·90
496	0431−134				2·40D		0·25			1·20
	0431−132	19			5·50X	1·4	0·8	0·48	0·76	0·99
754	0906−094		17:		1·10				1·72:	
1308	1130−037			2·3	2·30X		0·54		0·00	0·77
1620	1247−012		14:		0·84				1·79:	
1684	1306+107			2·9	1·63	0·54	0·28		0·69	0·93
1836	1358−113	10	13		4·40	1·9	1·1		0·59	0·73
2029	1508+059		24		2·66	0·8	0·2		1·40	1·32
2052	1514+072	126	140	54	28·0	5·2	2·3		0·99	1·33
2147	1559+158			8·4	4·66D	1·78	0·91		0·71	0·85
2382	2149−158		8·8		1·40X				1·17	
2448	2229−086		15		1·90X	0·60	0·45	0·20	1·32	0·79
2462	2236−176	16	14		4·20	1·5	1·2		0·80	0·69
2480	2243−178				0·84		0·21			0·73
2644	2338−001		11	3·5	1·62		0·38		1·22	0·77

In Table 4 the flux density spectral data are tabulated, together with two spectral indices α_- and α_+. The index α_- is the least squares fit to a power law ν^α for measurements made at frequencies 408 MHz and below, while α_+ is the corresponding index for frequencies 408 MHz and above. In the table, five of the 85 MHz flux densities are indicated as being uncertain by a colon. In these cases the coincidence between the 85 MHz positions and the present 408 MHz positions is not good, suggesting that extra emission has been included in the 50′ arc beam used at 85 MHz. Where the spectral index α_- depends on these measurements it has also been indicated as uncertain.

Mean indices have been calculated (excluding the uncertain results indicated by a colon) and they are as follows:

$$\langle\alpha_-\rangle = -1\cdot00\pm0\cdot12, \quad \langle\alpha_+\rangle = -0\cdot88\pm0\cdot05.$$

Neither of these is significantly different from the mean index of about $-0\cdot9$ obtained by Murdoch (1976) for various samples of sources selected at 408 MHz. Moreover, the differences which do exist are in the sense expected from the operation of selection effects in the finding surveys.

It has been suggested by Bridle and Feldman (1972) that steep-spectrum extended radio sources may be associated with X-ray emission as the result of inverse Compton scattering of the synchrotron electrons from the microwave background. No definite support for this suggestion could be found among the present results. One of the observed clusters A401, which is an X-ray source, has been advanced as an example of the suggested mechanism by Harris and Romanishin (1974). They attributed to it a steep-spectrum extended source which they found at low frequencies. In our observations there is no indication of low-level extended emission, but an unresolved radio source (4C 13.17), probably unassociated with the cluster, is located about half a degree north following 0255+133. A blending of these two sources may possibly have caused a misinterpretation of their results. In fact, any low resolution observations are subject to uncertainties of this type, and many published spectra should be treated with caution.

Only one clear example of an excessively extended source was found among the present observations. The cluster A194 contains a double source apparently surrounded by an extensive halo (Schilizzi and McAdam 1975). However, its spectrum is normal, and it does not appear to have been detected as an X-ray source.

The MSH catalogue (Mills *et al.* 1958) allows some further possibilities of search for extended steep-spectrum sources. Possible examples should be included among the Abell cluster associations suggested by Mills (1960). Those sources listed in Table 4 with uncertain 85 MHz flux densities may be in this category. Further examples not related to the sources found in the present investigation are located near the following clusters: A36, A477, A513, A538, A869, A1773, A2328, A2384, A2544, A2612. However, the probability of chance associations is such that there is no compelling reason to assume that any of these associations is physical. In fact, the evidence of the MSH survey would appear to severely limit the possibility of making a *positive* identification of steep-spectrum extended emission associated with any of the present sample of clusters south of declination $+10°$; in possible examples the observed flux densities are not much higher than the background confusion level.

8. Conclusions

The present observations of 247 Abell clusters show no clearly demonstrable peculiarities in the radio emission associated with the clusters. The properties of radio galaxies identified in the clusters appear to fall within the wide range of properties of other radio galaxies and no clear evidence for excess emission by the intergalactic matter could be found. We conclude that the presumed presence of excess intergalactic matter in the clusters has no marked effect on the development of radio galaxies, and it does not itself emit sufficiently to be differentiated with certainty from the normal fluctuations of sky brightness.

No clear examples of 'head–tail' sources were found, although 0445–206 and 1508 + 182 may be examples. With the resolution available, such sources would only be easily recognizable in very close clusters, and there are few of these in the sample. However, the rather large median displacement between the radio and optical centroids of identified galaxies may possibly represent a similar effect.

The most interesting result arises from the correlations with cluster richness. These seem to imply that the potentiality for radio emission is imprinted on a galaxy when it is formed as a result of some physical property associated with the primordial gas cloud.

Acknowledgments

The work was supported by the Australian Research Grants Committee, the University of Sydney Research Committee and the Science Foundation for Physics within the University of Sydney. One of us (D.G.H.) acknowledges receipt of a Commonwealth Postgraduate Research Award.

Note added in proof

Observations with the Fleurs synthesis telescope have indicated that 0445–206 is not a 'head–tail' source.

References

Abell, G. O. (1958). *Astrophys. J. Suppl. Ser.* **3**(31).
Abell, G. O. (1972). *In* 'External Galaxies and Quasi-Stellar Objects' (Ed. D. S. Evans), p. 341 (Reidel: Dordrecht).
Bautz, L. P., and Abell, G. O. (1973). *Astrophys. J.* **184**, 709.
Bolton, J. G., Shimmins, A. J., and Wall, J. V. (1975). *Aust. J. Phys. Astrophys. Suppl.* No. 34, 1.
Bridle, A. H., and Feldman, P. A. (1972). *Nature Phys. Sci.* **235**, 168.
Cameron, M. J. (1971). *Mon. Not. R. Astron. Soc.* **152**, 429.
Ekers, J. A. (1969). *Aust. J. Phys. Astrophys. Suppl.* No. 7.
Gower, J. F. R., Scott, P. F., and Wills, D. (1967). *Mem. R. Astron. Soc.* **71**, 49.
Harris, D. E., and Romanishin, W. (1974). *Astrophys. J.* **188**, 209.
Hunstead, R. W. (1971). *Mon. Not. R. Astron. Soc.* **152**, 277.
Hunstead, R. W. (1972). *Mon. Not. R. Astron. Soc.* **157**, 367.
Mills, B. Y. (1960). *Aust. J. Phys.* **13**, 550.
Mills, B. Y., Shobbrook, R. R., and Stewart-Richardson, D. (1968). *Aust. J. Phys.* **21**, 511.
Mills, B. Y., Slee, O. B., and Hill, E. R. (1958). *Aust. J. Phys.* **11**, 360.
Munro, R. E. B. (1971). *Aust. J. Phys.* **24**, 263.
Murdoch, H. S. (1976). *Mon. Not. R. Astron. Soc.* **177**, 441.
Noonan, T. W. (1973). *Astron J.* **78**, 26.
Rowan-Robinson, M. (1972). *Astron. J.* **77**, 543.
Sandage, A. (1972). *Astrophys. J.* **178**, 1.
Sargent, W. L. W. (1973). *Publ. Astron. Soc. Pac.* **85**, 281.
Schilizzi, R. T. (1975). *Mem. R. Astron. Soc.* **79**, 75.
Schilizzi, R. T., and McAdam, W. B. (1975). *Mem. R. Astron. Soc.* **79**, 1.
Sholomitskii, G. B. (1968*a*). *Sov. Astron.* **11**, 756.
Sholomitskii, G. B. (1968*b*). *Sov. Astron.* **12**, 381.
Slee, O. B., and Higgins, C. S. (1973). *Aust. J. Phys. Astrophys. Suppl.* No. 27.
Slee, O. B., and Higgins, C. S. (1975). *Aust. J. Phys. Astrophys. Suppl.* No. 36.
Wall, J. V., Shimmins, A. J., and Merkelijn, J. K. (1971). *Aust. J. Phys. Astrophys. Suppl.* No. 19.
Wall, J. V., Wright, A. E., and Bolton, J. G. (1976). *Aust. J. Phys. Astrophys. Suppl.* No. 39, 1.
Wyllie, D. V. (1969). *Mon. Not. R. Astron. Soc.* **142**, 229.

Appendix

Over the range of flux densities in which we are interested, we take the number of sources per steradian with flux density above S janskys to be given approximately by

$$n = 900\,S^{-1\cdot5}, \tag{A1}$$

The probability that a source of flux density S or greater is located within an angle θ of an arbitrary position is then given by

$$p = n\pi\theta^2 = 900\,\pi\,S^{-1\cdot5}\,\theta^2. \tag{A2}$$

To define a Category I source we determine θ_c from equation (2) (of the text) on putting $d = 0\cdot4$ Mpc, and we then determine S_c on putting $\theta = \theta_c$ and $p = 0\cdot02$ in equation (A2). The minimum luminosity $P_{\rm min}$ with which a cluster source will be classified as Category I is then given by substituting S_c in equation (3) of the text. On inserting the values of c and H_0 in S.I. units we obtain equation (4).

Manuscript received 11 February 1977